Available online at www.sciencedirect.com
ScienceDirect
Journal of Catalysis 254 (2008) 263–271
JOURNAL OF CATALYSIS
www.elsevier.com/locate/jcat

Improved catalytic activity using water for isomerization of linear butene to isobutene over heteropolyacid catalysts

Jin Zhang [a], Ryuichiro Ohnishi [b], Yuichi Kamiya [a], Toshio Okuhara [a,*]

[a] *Graduate School of Environmental Science, Hokkaido University, Sapporo 060-0810, Japan*
[b] *Japan Science and Technology Agency, 4-1-8 Honcho, Kawaguchi 332-0012, Japan*

Received 12 November 2007; revised 20 December 2007; accepted 25 December 2007

Available online 8 February 2008

Abstract

Water minimized a decrease in conversion for the isomerization of linear butene to isobutene on silica-supported heteropolyacid ($H_4SiW_{12}O_{40}$) catalysts while maintaining high selectivity toward isobutene. The role of water was related to surface acidic properties (number of surface acid sites and acid strength) and characteristics of hydrocarbon deposits (extent of deposits and hydrogen/carbon ratio), as determined by benzonitrile and ammonia temperature-programmed desorption as well as temperature-programmed oxidation of fresh and spent catalysts. It appears that highly unsaturated hydrocarbon deposits consisting of 8–12 carbon units covered surface acid sites, especially strong acid sites, limiting the isomerization reaction. Water in the feed was helpful in preserving the acid sites and decreasing the number of carbon units in the hydrocarbon deposits. Thus, conversion occurred more readily in the presence of water than in the absence of water.

Keywords: Skeletal isomerization; Linear butene; Isobutene; Water; Heteropolyacid; Hydrocarbon deposits; Temperature-programmed oxidation; Benzonitrile temperature-programmed desorption; Ammonia temperature-programmed desorption

1. Introduction

Linear butenes obtained from fluid catalytic cracking and steam cracking can be isomerized to isobutene, which is widely used as a raw material for such substances as polyisobutene, isobutyl-rubber, methacrolein, alkylated phenols, and methyl and ethyl *t*-butyl ether as octane number boosters. A large number of solid-acid catalysts have been tested to facilitate the skeletal isomerization of linear butenes to isobutene. Before 1993, solid acids used for this purpose were mainly in amorphous forms; related studies have been summarized by Choudhary [1] and Butler and Nicolaides [2]. After 1993, the focus of similar catalyst research changed because of commercial production involving skeletal isomerization by Shell and Lyondall using a ferrierite (FER) catalyst, a microporous zeolite with exceptionally high selectivity and stability [3]. The use of microporous materials as selective catalysts opened a completely new field of research. Studies have been conducted to identify other effective catalysts with microporosity and to explain the mechanism of the effectiveness of microporous catalysts. Reviews of these catalysts by Houzvicka and Ponec [4], Meriaudeau and Naccache [5], van Donk et al. [6], and Seo [7] explored factors that determine catalyst activity and selectivity, including pore structure, acid strength, acid site density, and role and location of coke. These studies also investigated reaction mechanisms, such as monomolecular, bimolecular, and pseudomonomolecular. Research published after these reviews has dealt with the reaction mechanism on FER-type zeolites [8–13] and new microporous catalysts [14–18].

The effect of water on catalytic performance during the isomerization of butenes has been investigated in research articles [19–23] and patents [24–28]. Szabo and Perrotey [19] and Gao and Moffat [22] reported that water added to the reaction medium stabilized the selectivity and activity on fluorinated alumina and boron phosphate catalysts; otherwise the selectivity and activity deteriorated with time. They attributed the increased stability to regeneration of acid sites by water, because Lewis acid sites on these catalysts are convertible to Brønsted

* Corresponding author. Fax: +1 81 011 706 4513.
E-mail address: oku@ees.hokudai.ac.jp (T. Okuhara).

0021-9517/$ – see front matter
doi:10.1016/j.jcat.2007.12.014

acid sites [29,30] in the presence of water. The patent literature [2,24–28] also describes an increase in catalyst stability and selectivity on fluorinated alumina, palladium-modified silica–alumina, and alumina catalysts; however, the authors of these patents attributed the increased stability and selectivity to a decrease in the amount of hydrocarbon deposits. Over tungsten oxide-based catalysts, the addition of water was detrimental to selectivity and/or activity [20,21,23].

Heteropolyacids promote a wide variety of acid-catalyzed reactions [31,32]. The acid strength and number of acid sites in heteropolyacids can be controlled by structure, metal composition, type of support, and pretreatment conditions. Solid heteropolyacids such as $H_3PM_{12}O_{40}$ and $H_4SiM_{12}O_{40}$ (M = W, Mo) are pure Brønsted acids. Okuhara et al. [33] measured the acid strength of heteropolyacids using Hammett indicators and concluded that solid $H_3PW_{12}O_{40}$ is a stronger acid than silica–alumina and HZSM-5 but is weaker than sulfated zirconia. We have reported [34–36] that C4–C7 linear alkanes are isomerized to corresponding branched alkanes with high selectivity and high stability over palladium–$H_4SiW_{12}O_{40}$–silica catalyst in the presence of hydrogen. Here hydrogen controls the concentration of alkenes to facilitate skeletal isomerization through a monomolecular mechanism while suppressing dimerization and polymerization.

Gao and Moffat [37] reported the isomerization of 1-butene to isobutene over $H_3PW_{12}O_{40}$–silica catalyst, although the yield of isobutene decreased with time. This decrease may be not surprising given the indication of polymer formation from infrared spectroscopic analysis of adsorbed 1- or *cis*-2-butene over $H_3PW_{12}O_{40}$–silica catalyst [38]. We expected that water might remove a part of adsorbed butene molecules from the catalyst surface and thereby suppress harmful polymer formation. The removal of adsorbed butene with water also may facilitate regeneration of acid sites. Bardin and Davis [39] had suggested the regeneration of acid sites based on the finding that treatment of $H_3PW_{12}O_{40}$–silica catalyst with water recovered activity for the double-bond isomerization of 1-butene.

In this paper, we demonstrate that the stability of catalytic activity is improved by water over $H_4SiW_{12}O_{40}$–silica catalysts. To clarify the role of water, we conducted detailed characterizations of the acidic features, hydrocarbon deposits, and structures of fresh and spent catalysts using ammonia and benzonitrile temperature-programmed desorption (TPD), temperature-programmed oxidation (TPO), and infrared spectroscopy. We also made surface area measurements. Here, ammonia is strongly basic (donor number = 34 kcal mol^{-1}, gas phase basicity = 819 kcal mol^{-1}), whereas benzonitrile is mildly basic (donor number = 11.9 kcal mol^{-1}, gas phase basicity = 781 kcal mol^{-1}) [40,41]. Results were compared with the catalytic performance in the presence and absence of water.

2. Experimental

2.1. Catalysts

A heteropolyacid of $H_4SiW_{12}O_{40}$ (abbreviated as H4SiW) was supported on two types of silica by an incipient wetness method, as reported previously [34–36]. The silicas used were Aerosil 300 (274 m^2 g^{-1}, Nippon Aerosil Co., Ltd.) and FSM-16 (1005 m^2 g^{-1}, Toyota Central R&D Labs, Inc.). Different amounts of H4SiW (in the range of 5–60 wt%) were loaded on Aerosil 300 and FSM-16 by changing the concentration of H4SiW in water. (Aerosil 300- and FSM-16-supported H4SiW are abbreviated as H4SiW/A300 and H4SiW/FSM16, respectively.) Partial neutralization of H4SiW with lithium was accomplished by titration, during which an aqueous solution of lithium carbonate was added dropwise to an aqueous solution of H4SiW with vigorous stirring at ambient temperature, as described previously [42,43]. Lithium-exchanged H4SiW on Aerosil 300 (15 wt% loading; abbreviated as LixH4-xSiW/A300) was prepared. All heteropolyacid catalysts were calcined at 523 K for 5 h in air.

FER having SiO_2/Al_2O_3 = 17.5, 64, and 93 (Tosoh Co.) were used as reference catalysts.

2.2. Catalytic reaction

The isomerization of linear butene to isobutene was performed in a continuous-flow fixed-bed reactor (quartz pipe, 4 mm i.d.) at 523–623 K under atmospheric pressure. The catalyst (0.1 g) was charged on quartz wool in the reactor, located at the center of a cylindrical furnace. The furnace temperature was controlled with a thermocouple placed outside the reactor and close to the catalyst bed. The tip of the thermocouple and the reactor were wrapped in nickel tape to ensure a homogeneous temperature. A reactant gas mixture of 7.4% 1-butene (Sumitomo Seika Chemicals Co. or Takachiho Chemical Ind. Co.) in helium (ultra pure; Japan Air Gases Ltd.) was fed at a total flow rate of 20.8 ml min^{-1} using two mass flow controllers (Kofloc FCC-3000-GI and Brooks 5850E) on the catalyst. For some experiments, water vapor was added in the reactant gas mixture. Helium was passed through a water bubbler, which was maintained at 355 K to supply water vapor into the reactant gas mixture. The amount of water supplied was approximately 5% of the reactant gas mixture, estimated from the decreasing weight of water in the bubbler after 10 h. The remainder of the reaction system after the water bubbler was heated to above 373 K.

The composition of reaction products at the outlet of the reactor was analyzed every hour by an online gas chromatograph (Shimadzu GC-14B), equipped with a flame ionization detector (FID) and a capillary column (CP-Al_2O_3/KCl PLOT, 25 m × 0.25 mm). The reaction products were identified using authentic samples. The molar fraction of a particular compound, j, in carbon base can be calculated from $A_j/\sum A_i$, where A_j is the area under the curve of the compound in the GC chromatogram (with the area essentially proportional to the carbon number of the compound). Catalytic performance was expressed as conversion and selectivity toward isobutene, defined as

$$\text{conversion} = \frac{\sum A_i\,(i \neq \text{linear butenes})}{\sum A_i} \times 100\%$$

and

$$\text{selectivity to isobutene} = \frac{A_{\text{isobutene}}}{\sum A_i\,(i \neq \text{linear butenes})} \times 100\%.$$

Here all linear butenes (1-, *cis*-2-, and *trans*-2-butene) were classified as reactants and were excluded from the summation, as indicated by $i \neq$ linear butenes, because the three linear butenes are easily converted to one another and reached equilibrium at the early stage of the reaction. Selectivity toward other byproducts, such as C3, butane, C5, and C8, also was calculated.

2.3. Other measurements

Benzonitrile (BN) TPD profiles were obtained using a homemade TPD system, equipped with an FID. After pretreatment at 523 K under nitrogen flow (40 ml min^{-1}), the catalyst was exposed to 0.122 μmol h^{-1} of BN at 373 K for 1 h, and the excess BN was removed at 373–393 K. The flow rates of BN and nitrogen were controlled by a syringe pump (Econoflo; Harvard Apparatus Inc.) and a mass flow controller (Brooks 5850E). Temperature of the catalyst was increased at a rate of 10 K min^{-1} to 973 K under nitrogen flow while monitoring the FID signal of the exit gas. The spectrum of BN-TPD was deconvoluted using a peak-fitting program, Fityk, provided that the spectrum was composed of several peaks with Gaussian function. Then peak parameters, such as area, position, and width, were evaluated. The amount of BN adsorbed in mol g^{-1} was calculated from the area calibrated by a sensitivity factor, obtained from the feed rate of BN and FID signal at the saturation of BN adsorption.

Ammonia (NH_3)-TPD profiles were obtained by a multitask TPD system (BEL Japan), equipped with a quadrupole mass spectrometer (ANELVA; M-QA100S). After pretreatment at 523 K under helium flow, the catalyst was exposed to NH_3 of 13 kPa at 373 K for 20 min, and the excess NH_3 was removed under helium flow at 373 K for 0.5 h. The temperature of the sample was increased at a rate of 10 K min^{-1} to 973 K, and the desorbed gas was monitored at $m/z = 16$. The NH_3-TPD spectrum was analyzed in a manner similar to that of BN-TPD. The amount of NH_3 desorbed in mol g^{-1} was calculated from the area calibrated by a sensitivity factor, obtained from the peak area of NH_3-TPD of H-ZSM-5 and its number of acid sites. The acid amount was obtained from the sum of peak areas excluding a peak located below 460 K, which originated from weakly held NH_3 [44].

TPO of spent catalyst used for 10 h in the reaction was conducted using a homemade TPD system, equipped with a quadrupole mass spectrometer (Anelva, M-200QA-M). The catalyst temperature was increased at a rate of 10 K min^{-1} to 973 K under a 10% oxygen–helium flow. The mass spectrum of the exit gas was obtained by multiple-ion monitoring mode at $m/z = 18$ for water, 28 for CO, and 44 for CO_2. The mass number of 32 also was monitored to check the availability of oxygen in the stream. Absolute sensitivity factors for water, CO, and CO_2 were obtained from plots of mass peak height against concentration of gas mixture of water and helium, CO and helium, and CO_2 and helium. Desorption rates were calculated from the product of peak height and absolute sensitivity factor.

Fourier transform infrared spectra (FTIR) of the catalysts were recorded using potassium bromide (KBr) disks containing 1 wt% catalyst using a spectrometer (FT/IR 230, JASCO) at room temperature. The BET surface area was determined from a nitrogen adsorption isotherm at liquid nitrogen temperature using a BELSORP 28SA instrument (BEL Japan Inc.).

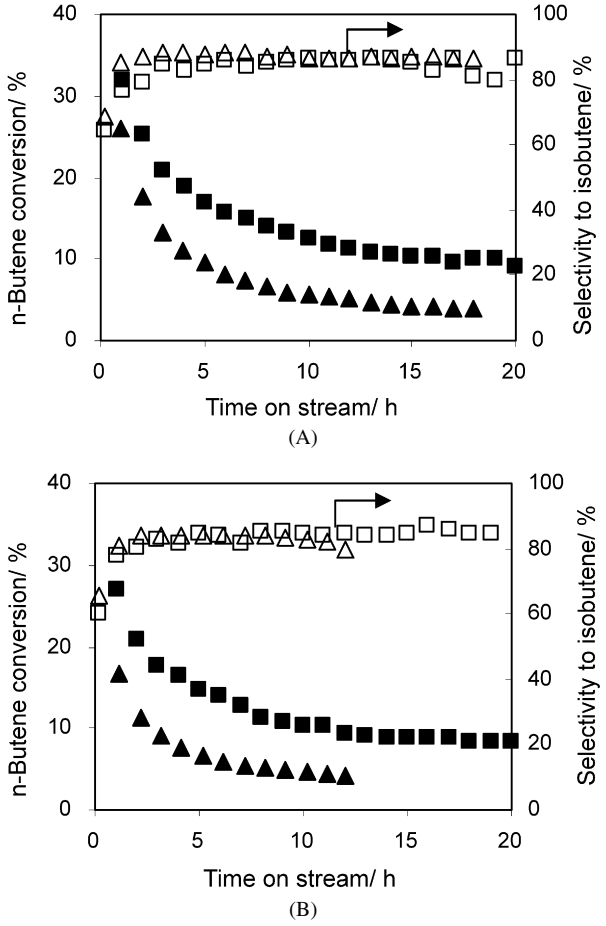

Fig. 1. Time course of conversion (▲, ■) and selectivity (△, □) in the presence (■, □) and absence (▲, △) of water at 593 K on (A) 40 and (B) 20 wt% H4SiW/A300.

3. Results and discussion

3.1. Skeletal isomerization of linear butene to isobutene

Figs. 1A and 1B show the time course of conversion and selectivity toward isobutene on 20 and 40 wt% H4SiW/A300 catalysts. Initial high conversion on both catalysts declined with time; however, water increased the conversion level. As a result, conversion at 10 h in the presence of water was about twice as great as that in the absence of water. In contrast to this conversion, the time course of selectivity toward isobutene in the absence of water changed in a manner similar to that in the presence of water, that is, from initial low selectivity (60%) to >80% selectivity. Such an increase in selectivity was observed on all catalysts examined. The main byproducts were butane, pentenes, and octenes, suggesting that these byproducts and isobutene remnants are produced through dimerization of linear butenes, isomerization, and cracking. Fig. 2 shows the change in catalyst performance when water was introduced to

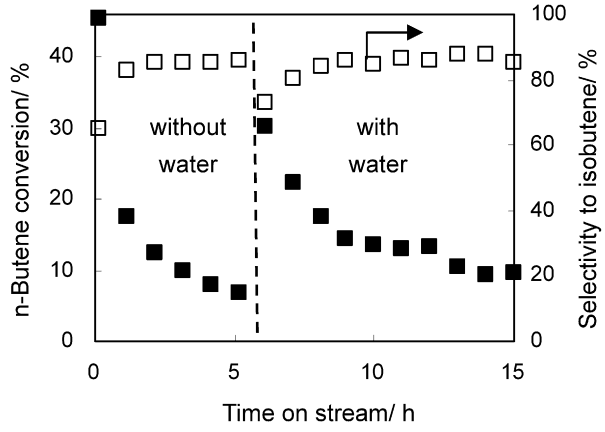

Fig. 2. Change in conversion (■) and selectivity (□) with water addition on 40 wt% H4SiW/A300 at 593 K.

the reactant gas mixture in the middle of the reaction. The introduction of water led to dramatically increased conversion. This sudden increase in conversion suggests that water expelled adsorbed hydrocarbons from catalyst surface. Accordingly, water may partly restore the original activity of acid sites, as suggested by Bardin and Davis [39]. In addition, water will reduce the surface concentration of hydrocarbons and hinder polymer formation, resulting in hydrocarbon deposits. The lower surface concentration of hydrocarbons may explain the greater stable conversion in the presence of water compared with that in the absence of water.

Figs. 3A and 3B show plots of stable conversions and selectivities after 10 h against loading amounts of H4SiW in H4SiW/A300 and H4SiW/FSM16 in the presence and absence of water. These figures demonstrate the significantly improved conversion in the presence of water while maintaining high selectivity toward isobutene (>80%). Stable conversion in the presence and absence of water increased with H4SiW loading, and then decreased. Maximum conversions on H4SiW/FSM16 were 12.3% in the presence of water and 8.8% in the absence of water, whereas those on HSiW/A300 were 11.3 and 5.6%, respectively. The FSM-16-supported catalyst gave a slightly greater conversion compared with the Aerosil 300-supported catalyst.

Table 1 presents stable conversions and selectivities of various catalysts. Note that the stable conversion of FER ($SiO_2/Al_2O_3 = 64$) was not improved with water but instead decreased. Similarly, water did not improve the conversion of other FERs ($SiO_2/Al_2O_3 = 17.5$ and 93) (data not shown). The 15 wt% Li0.05H3.95SiW/A300 and Li0.2H3.8SiW/A300 gave stable conversions similar to that of the parent 15 wt% H4SiW/A300 in the presence of water.

3.2. Acidic characteristics of fresh and spent catalysts

We measured the acidic characteristics of catalysts using two methods, BN-TPD and NH_3-TPD, and compared these characteristics with catalytic performance.

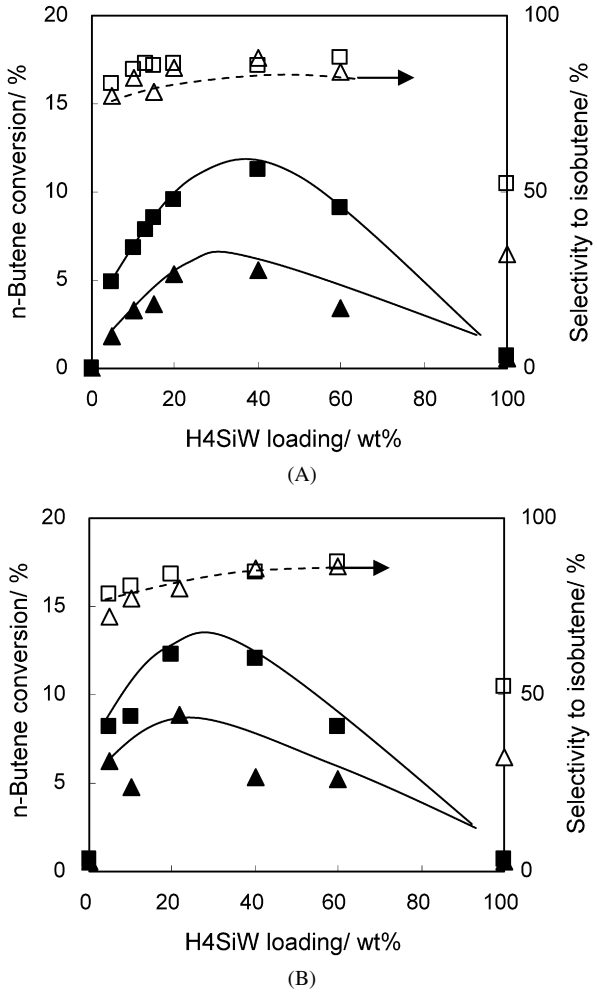

Fig. 3. Stable conversion (▲, ■) and selectivity (△, □) in the presence (■, □) and absence (▲, △) of water at 593 K on (A) H4SiW/A300 and (B) H4SiW/FSM16 with various H4SiW loadings.

Table 1
Conversion of linear butene and selectivity toward isobutene on various catalysts at 593 K

Catalyst	Water presence	Conversion[a] (%)	Ratio[b]	Selectivity[a] (%)
40 wt% H4SiW/A300	No	6	2.0	88
40 wt% H4SiW/A300	Yes	11		86
40 wt% H4SiW/FSM16	No	5	2.3	86
40 wt% H4SiW/FSM16	Yes	12		85
FER ($SiO_2/Al_2O_3 = 64$)	No	16	0.7	86
FER ($SiO_2/Al_2O_3 = 64$)	Yes	11		82
15 wt% H4SiW/A300	Yes	8		86
15 wt% Li0.05H3.95SiW/A300	Yes	9		72
15 wt% Li 0.2H3.95SiW/A300	Yes	9		84
15 wt% Li0.4H3.95SiW/A300	Yes	7		88

[a] Stable conversion and selectivity toward isobutene in carbon base.
[b] Ratio of conversion in the presence of water to that in the absence of water.

3.2.1. BN-TPD

Fig. 4 shows BN-TPD spectra of fresh H4SiW/FSM16 with various H4SiW loadings. Corresponding BN-TPD spectra of

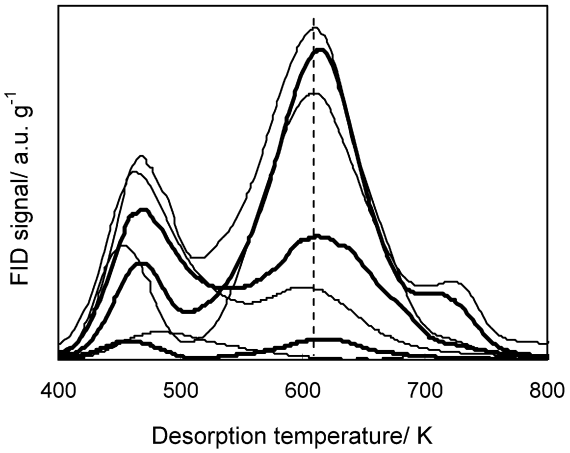

Fig. 4. BN-TPD spectra of fresh H4SiW/FSM16 with various H4SiW loadings. Loading of H4SiW (broken line) (from top to bottom): 20, 40, 60, 10, 5, 100 (×4) and 0 wt%.

fresh H4SiW/A300 have been reported previously [36]. Three distinct peaks were observed at approximately 460, 610, and 720 K and were deconvoluted using a peak-fitting program. The peak at 460 K is due to physically adsorbed BN, because the peak temperature is close to its boiling point of 463.9 K. Therefore, the total acid amount was estimated from the sum of peak areas at 610 and 720 K. Fig. 5A shows the estimated total acid amounts of H4SiW/FSM16 and H4SiW/A300, which attained a maximum at approximately 20 and 40 wt% loading of H4SiW, and then decreased. Silica, of both Aerosil 300 and FSM-16, demonstrated no peak in BN-TPD, except for a small peak at 480 K. The decreased amount of acid at high H4SiW loadings may be due to a decrease in surface area, as shown in Fig. 5B. These results indicate that BN adsorbs only on acid sites on the upper surface and does not absorb into the bulk of H4SiW.

The conversion increased, attained a maximum, and then decreased with H4SiW loading, similar to the amount of acid. Thus, we plotted conversion against acid amount and found that conversion increased progressively with the amount of acid in H4SiW/FSM16 and H4SiW/A300 (data not shown). These results reconfirm that skeletal isomerization is catalyzed by acid sites.

Table 2 shows the acid amounts derived from two peaks at 610 and 720 K, along with their sums on fresh and spent catalysts used in the absence and presence of water. The total acid amount decreased to less than half of the original value after the reaction. In particular, the acid sites from the peak at 720 K were barely observable on the spent catalysts, suggesting preferential poisoning of stronger acid sites over weaker acid sites. Note that water in the reactant feed helped prevent the deterioration of acid sites.

3.2.2. Ammonia (NH_3)-TPD

NH_3-TPD spectra appeared very different from BN-TPD profiles. Fig. 6 shows NH_3-TPD spectra of fresh H4SiW/FSM16 with various H4SiW loadings. Corresponding NH_3-TPD spectra of fresh H4SiW/A300 have been reported previously [36]. The amounts of chemically adsorbed NH_3 on

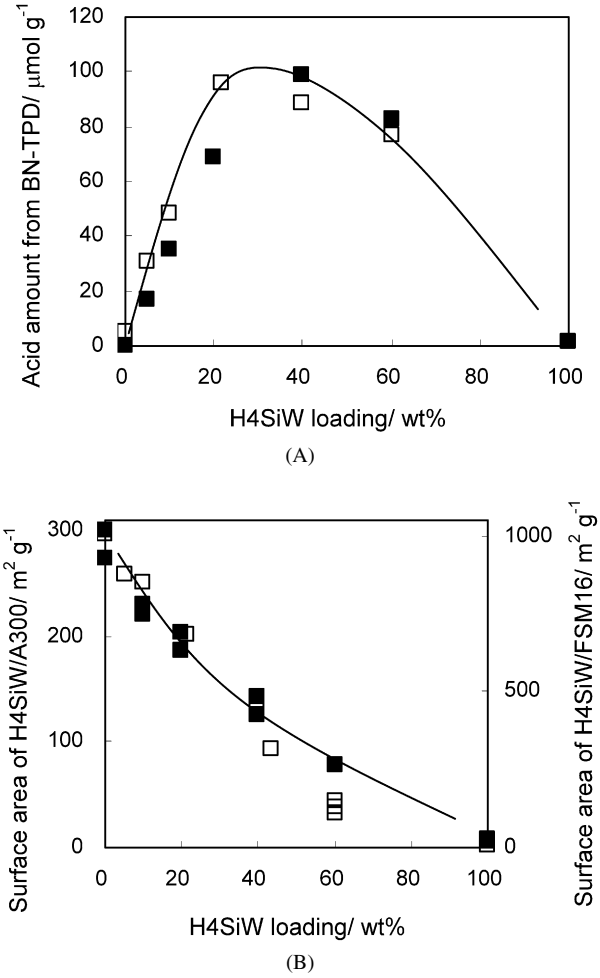

Fig. 5. Change in (A) acid amount estimated from BN-TPD and (B) surface area with H4SiW loadings on Aerosil 300 (■) and FSM-16 (□).

Table 2
Acid amount estimated from BN-TPD of fresh and spent catalysts with various H4SiW loadings on Aerosil 300

H4SiW loading (wt%)	Acid amount[a] (μmol g^{-1})		
	Fresh	Spent, no water[b]	Spent, with water[b]
10	34.8 (33.5, 1.3)	17.0 (17.0, 0.0)	18.3 (18.3, 0.0)
20	68.7 (60.6, 8.1)	15.0 (15.0, 0.0)	27.5 (27.5, 0.0)
40	85.3 (77.9, 7.4)	18.8 (18.8, 0.0)	26.8 (26.8, 0.0)
60	82.9 (65.7, 17.1)	5.4 (4.6, 0.8)	0.9 (0.8, 0.1)

[a] Total acid amount (acid amount from peak at 610 K, acid amount from peak at 720 K).
[b] Used for 10 h at 593 K in the absence and presence of water.

catalyst were estimated from the spectra and plotted against H4SiW loading, as shown in Fig. 7. Regardless of the support, the amount of NH_3 chemically adsorbed on the catalyst increased linearly with H4SiW loading. In addition, a line depicting the number of protons in the catalyst coincided with the amount of NH_3 chemically adsorbed on the catalyst. These results demonstrate that NH_3 not only adsorbs onto the catalyst surface, but also is absorbed into the H4SiW bulk. Thus, NH_3 interacts with all of the protons in H4SiW on silica. In contrast,

BN could adsorb only onto the catalyst surface, as described previously.

The spectrum of pure H4SiW contained a sharp peak at 810 K, whereas the spectra of H4SiW/FSM16 consisted of broad and poorly separated peaks near 680, 600, and 450 K. In contrast, the spectra of H4SiW/A300 with >40 wt% loading exhibited a sharp peak at 770–810 K in addition to those poorly separated peaks, as shown by the 40 and 60 wt% H4SiW/A300 (see Ref. [36] and Fig. 8B). These results suggest a greater dispersion of H4SiW on FSM-16 than on Aerosil 300, probably due to the threefold-greater surface area of FSM-16 compared with Aerosil 300.

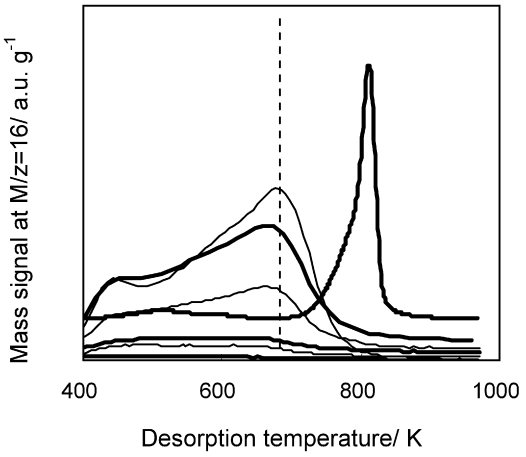

Fig. 6. NH_3-TPD spectra of fresh H4SiW/FSM16 with various H4SiW loadings. Loadings of H4SiW (broken line) (from top to bottom): 60, 40, 22, 100 (×0.5), 10, 5, and 0 wt%.

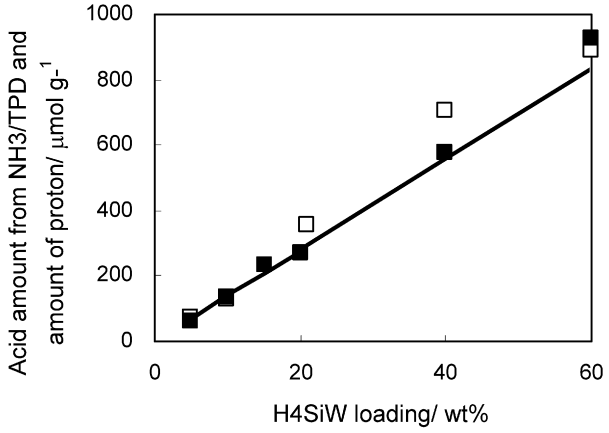

Fig. 7. Change in proton amount (line) and acid amounts estimated from NH_3-TPD with H4SiW loadings on Aerosil 300 (■) and FSM-16 (□).

Spent catalysts used in the absence of water were subjected to NH_3-TPD measurements as well. Figs. 8A, 8B and 8C compare the NH_3-TPD spectra obtained from fresh and spent catalysts of 20 wt% H4SiW/A300, 40 wt% H4SiW/A300, and 40 wt% H4SiW/FSM16. The NH_3-TPD spectra of fresh and spent 20 wt% H4SiW/A300 were similar to those of 40 wt% H4SiW/FSM16, which contained peaks at 480, 550, and 650–680 K. Although quantitative analysis of the spectra was difficult because of overlapping peaks, it appears that the height of the peak at 650–680 K for the spent catalyst decreased dramatically, whereas that at 480 K, attributed to hydrogen-bonded NH_3 [44], increased compared with the peaks of the fresh catalyst. The height of the peak at 550 K decreased slightly. These results indicate that the stronger acid sites are more susceptible to poisoning during the reaction, in agreement with the BN-TPD measurements. In contrast, it appeared that a sharp peak at 770 K on the 40 wt% H4SiW/A300 was less susceptible to poisoning than the peaks at 600–700 K, as shown in Fig. 8B. This indicates that the peak at 770 K comes from the H4SiW bulk, where reactants could not reach the protons.

3.2.3. Relation between catalytic performance and acidic characteristics

Our findings confirm that the skeletal isomerization of linear butene to isobutene is catalyzed by acid sites, where the conversion of linear butene increased progressively with the number of surface acid sites of H4SiW/FSM16 and H4SiW/A300 catalysts with various H4SiW loadings, as measured by BN-TPD (Figs. 3 and 5). Strong acid sites exposed on the catalyst surface were lost during the reaction. Weak acid sites and acid sites in H4SiW bulk were more durable than strong acid sites exposed

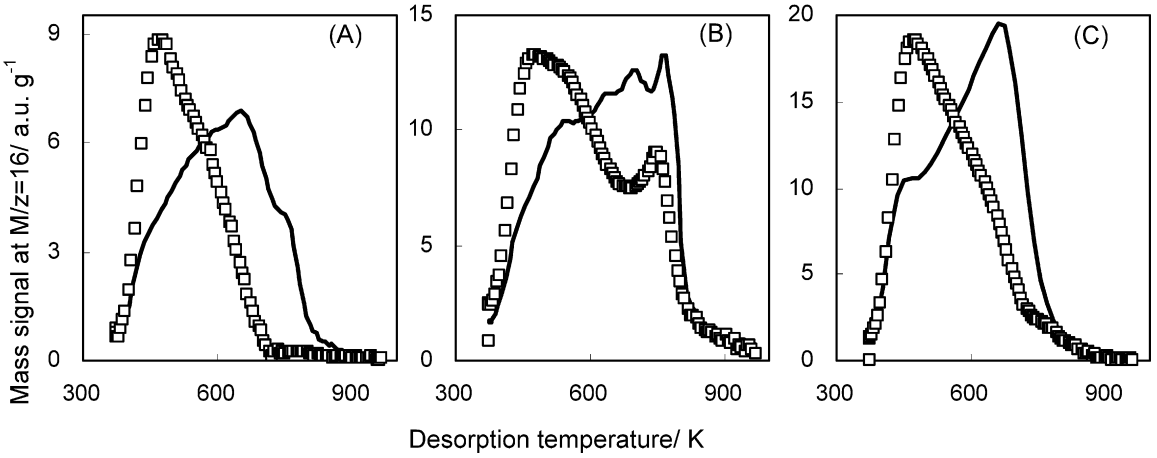

Fig. 8. NH_3-TPD spectra of fresh catalyst (line) and spent catalyst in the absence of water (□) for (A) 20 wt% H4SiW/A300, (B) 40 wt% H4SiW/A300, and (C) 40 wt% H4SiW/FSM16.

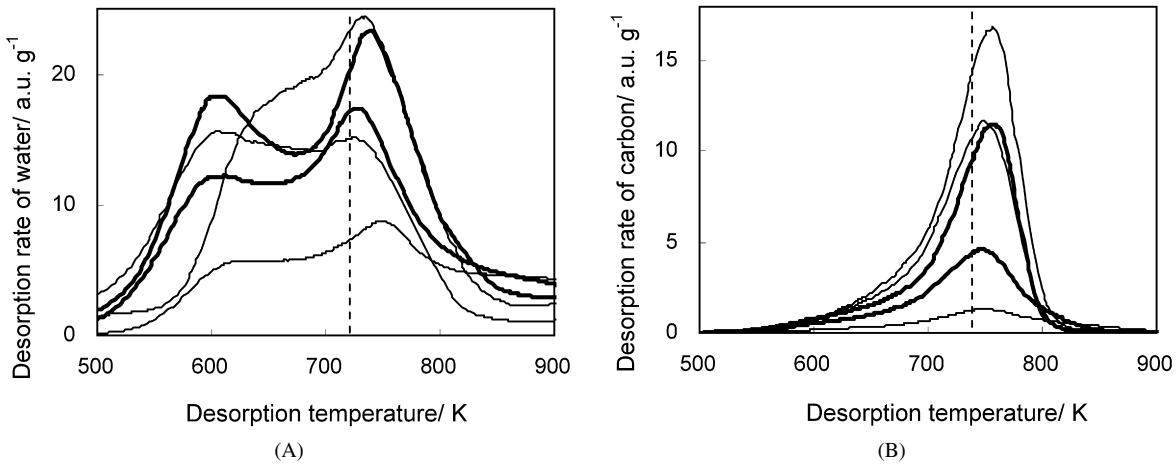

(A) (B)

Fig. 9. Desorption rates of (A) water and (B) carbon (=CO + CO_2) estimated from TPO spectra of spent H4SiW/A300 catalysts used in the absence of water. Loadings of H4SiW (broken line) (from top to bottom): (A) 40, 20, 10, 60, 5 and (B) 40, 60, 20, 10, and 5 wt%.

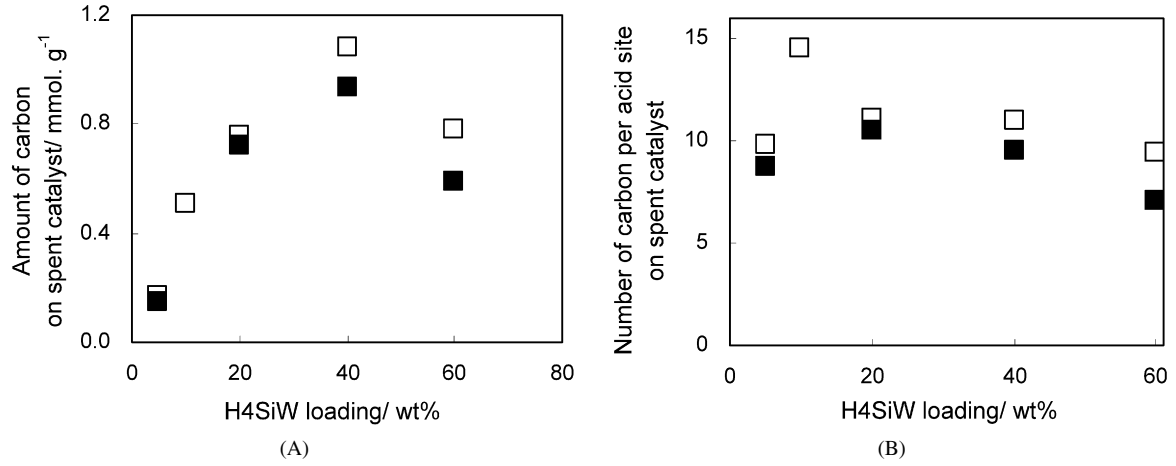

(A) (B)

Fig. 10. Change in (A) amount of carbon and (B) carbon chain length per acid site on spent catalysts used in the absence (□) and presence (■) of water with H4SiW loading.

on the catalyst surface, as shown in Table 2 and Fig. 8. Catalytic activity declined with time because of a decrease in acid sites, especially strong acid sites. Water vapor was helpful in preserving the acid sites during the reaction, as shown in Table 2.

3.3. TPO of spent catalysts

As described previously, both conversion and the number of acid sites decreased with time, probably because of the accumulation of hydrocarbon deposits on the catalyst surface. Accordingly, we conducted TPO of the spent catalysts to identify the characteristics of the hydrocarbon deposits formed during the reaction.

Desorption rates of carbon and water were calculated from TPO spectra at $m/e = 18$, 28, and 44 of spent catalysts used in the absence of water. Fig. 9 shows those desorption spectra on H4SiW/A300 catalysts with various H4SiW loadings. A sole peak occurred at 750–760 K in the carbon desorption spectra, whereas two or more peaks could be seen in the water desorption spectra. The amount of carbon estimated from the peak area of carbon desorption spectra increased with H4SiW loading, reached a plateau at 20–40 wt% loading, and then decreased, as shown in Fig. 10A. Comparing Fig. 10A with Figs. 3 and 5A indicates that the conversion of linear butene and the amount of carbon in hydrocarbon deposits first increased and then decreased with H4SiW loading in a manner similar to the number of acid sites. These results indicate that the formation reaction of hydrocarbon deposit and skeletal isomerization of linear butene are acid-catalyzed reactions and may share a common intermediate. It should be noted that the amount of carbon in the presence of water was always smaller than that in the absence of water, although the differences were small.

Knowing the amount of carbon in hydrocarbon deposits and the acid amount from BN-TPD on fresh catalysts allowed calculation of an average carbon number of hydrocarbon deposits adsorbed on one acid site, as shown in Fig. 10B. It appears that hydrocarbon deposits were derived from a dimer or trimer of butene (carbon number 8–12). In addition, the average carbon numbers of hydrocarbon deposits in the presence of water were smaller than those in the absence of water.

Fig. 11 shows the hydrogen/carbon (H/C) ratio in hydrocarbon deposits estimated from the ratio of peak height in a water

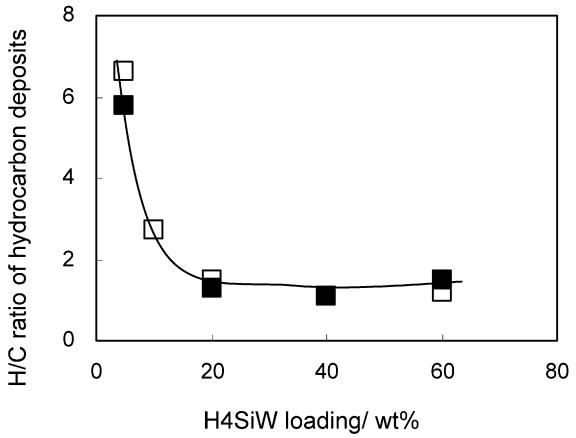

Fig. 11. Change in H/C ratio of hydrocarbon deposits on spent catalysts used in the absence (□) and presence (■) of water with H4SiW loading.

desorption spectrum to that in a carbon spectrum at the peak position of 750–760 K. This ratio represents the highest possible value, because the desorbed water will come not only from hydrocarbon deposits, but also from bound water and decomposition of heteropolyacid. A high initial H/C ratio decreased with increasing H4SiW loading and then became stable at 1.0–1.5 at loadings >20 wt% H4SiW. This ratio suggests that the hydrocarbon deposits were highly unsaturated in nature, because the ratios of monoalkenes and of condensed aromatics were 2 and <1, respectively.

3.4. FTIR measurements of fresh and spent catalysts

To check whether the heteropolyacid structure decomposed during the reaction, FTIR measurements were obtained on fresh and spent catalysts used in the presence of water. Figs. 12A and 12B compare fresh and spent catalysts. Four distinct peaks were observed on fresh H4SiW/A300 at 977–982, 928–930, 884–886, and 785–813 cm^{-1}, which have been assigned to the vibrational modes of W=O, Si–O, W–O, and W–O, respectively, in Keggin anions [31]. The final peak at 785 cm^{-1} progressively shifted to higher wavenumbers with decreasing H4SiW loading due to overlap with a Si–O peak of silica at 818 cm^{-1}. Fig. 12 shows no significant difference between fresh and spent catalysts, indicating no decomposition of heteropoly Keggin anion structure during reaction in the presence of water.

4. Conclusion

The skeletal isomerization of linear butene to isobutene was conducted at 593 K on silica (Aerosil 300 or FSM-16)-supported $H_4SiW_{12}O_{40}$ and other solid-acid catalysts in the presence and absence of water. Although the initial high activity declined with time, water minimized the decrease. At 10 h, stable conversion in the presence of water was approximately twice that in the absence of water while high selectivity (>80%) to isobutene was maintained. In contrast, stable conversion on FER (SiO_2/Al_2O_3 = 17.5, 64, and 93) did not improve with water addition, but rather decreased.

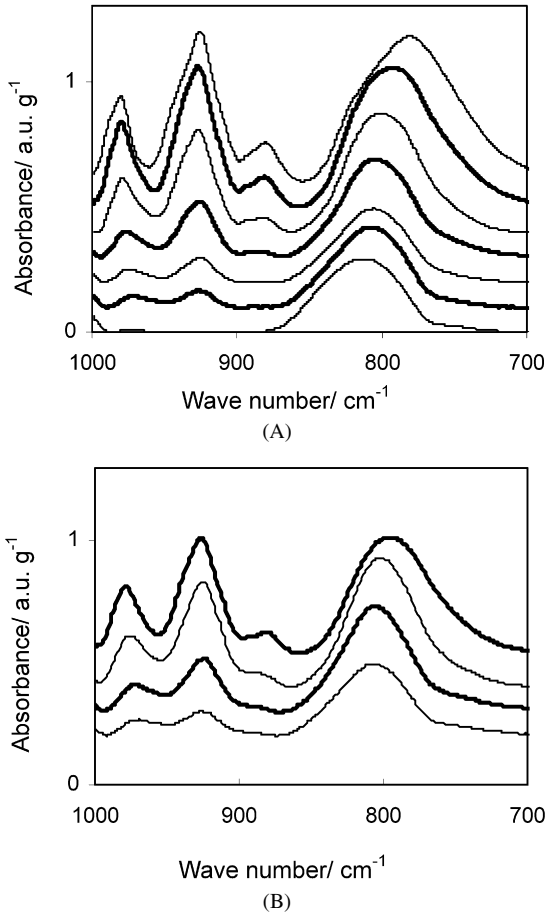

Fig. 12. FTIR spectra of (A) fresh H4SiW/A300 and (B) spent H4SiW/A300 used in the presence of water with various H4SiW loadings. Loadings of H4SiW (from top to bottom): (A) 100, 60, 40, 20, 10, 5, 0 and (B) 60, 40, 20, and 10 wt%.

Stable conversion increased up to 20 or 40 wt% loading of $H_4SiW_{12}O_{40}$ on silica and then decreased, whereas stable selectivity toward isobutene was as high as 80%. A similar trend with a loading amount of $H_4SiW_{12}O_{40}$ was observed for the amounts of hydrocarbon deposits and surface acid, as measured by TPO and BN-TPD. These results indicate that both formation of hydrocarbon deposits and skeletal isomerization of linear butene were catalyzed by acid sites and may share a common intermediate.

BN-TPD and NH_3-TPD of fresh and spent catalysts demonstrated that strong acid sites exposed on the catalyst surface were lost preferentially during the reaction, whereas weak acid sites and those in $H_4SiW_{12}O_{40}$ bulk were more durable. Because hydrocarbon deposits cover the acid sites, they are poisoned during the reaction, especially the strong acid sites. This explains the decrease in conversion. Furthermore, it appears that hydrocarbon deposits are composed of butene dimers or trimers and are highly unsaturated in nature, determined from TPO analysis of spent catalysts. FTIR measurements revealed no decomposition of heteropolyacid structure during the reaction in the presence of water.

According to BN-TPD, NH_3-TPD, and TPO measurements, the presence of water was helpful in preserving acid sites and

lowering the average carbon numbers of hydrocarbon deposits on one acid site. Furthermore, conversion increased dramatically as soon as water was introduced into the system, suggesting substitution of water for a portion of adsorbed hydrocarbons at the catalyst surface, leading to increased activity of acid sites and decreased surface concentration of hydrocarbons. These results explain the greater stable conversion in the presence of water than in the absence of water.

Acknowledgments

Financial support was provided by a grant from Core Research for Evolutional Science and Technology from the Japan Science and Technology Agency.

References

[1] V.R. Choudhary, Ind. Eng. Chem. Prod. Res. Dev. 16 (1977) 12.
[2] A.C. Butler, C.P. Nicolaides, Catal. Today 18 (1993) 443.
[3] P. Grandvallet, K.P. de Jong, H.H. Mooiweer, A.G.T. Kortbeek, B. Kraushaar-Czarnetzki, European Patent 0 501 577, 1992, to Shell Int. Res.
[4] J. Houzvicka, V. Ponec, Catal. Rev. Sci. Eng. 39 (1997) 319.
[5] P. Meriaudeau, C. Naccache, Adv. Catal. 44 (1999) 505.
[6] S. van Donk, J.H. Bitter, K.P. de Jong, Appl. Catal. A 212 (2001) 97.
[7] G. Seo, Catal. Surv. Asia 9 (2005) 139.
[8] P. Canizares, A. Carrero, Appl. Catal. A 248 (2003) 227.
[9] G. Onyestyak, J. Valyon, G. Pal-Borbely, L.V.C. Rees, Stud. Surf. Sci. Catal. 154 (2004) 2316.
[10] B. de Menorval, P. Ayrault, N.S. Gnep, M. Guisnet, J. Catal. 230 (2005) 38.
[11] A.G. Stepanov, S.S. Arzumanov, M.V. Luzgin, H. Ernst, D. Freudeet, J. Catal. 229 (2005) 243.
[12] M. Kangas, J. Villegas, N. Kumar, T. Salmi, D.Y. Murzin, F. Sandelin, E. Harlin, Catal. Today 100 (2005) 363.
[13] B. de Menorval, P. Ayrault, N.S. Gnep, M. Guisnet, Appl. Catal. A 304 (2006) 1.
[14] F.J. Maldonado-Hódar, A.F. Pérez-Cadenas, J.L.G. Fierro, C. Moreno-Castilla, J. Phys. Chem. B 107 (2003) 5003.
[15] S.H. Lee, D.K. Lee, C.H. Shin, Y.K. Park, P.A. Wright, W.M. Lee, S.B. Hong, J. Catal. 215 (2003) 151.
[16] Y.W. Suh, J.W. Lee, H.K. Rhee, Appl. Catal. A 274 (2004) 159.
[17] Y.C. Shang, W.X. Zhang, T. Li, T.H. Wu, Chin. J. Catal. 25 (2004) 158.
[18] Y.C. Shang, W.X. Zhang, M.J. Jia, P.P. Yang, D.Z. Jiang, T.H. Wu, React. Kinet. Catal. 85 (2005) 245.
[19] J. Szabo, J. Perrotey, J. Mol. Catal. 67 (1991) 79.
[20] Z.X. Cheng, V. Ponec, Catal. Lett. 25 (1994) 337.
[21] L.H. Gielgens, M.G.H. Vankampen, M.M. Broek, R. Vanhardeveld, V. Ponec, J. Catal. 154 (1995) 201.
[22] S. Gao, J.B. Moffat, J. Catal. 180 (1998) 142.
[23] M.A. Alvarez-Merino, F. Carrasco-Marin, C. Moreno-Castilla, J. Catal. 192 (2000) 374.
[24] B. Juguin, J. Miquel, FR Patent 2484400, 1981, to Institut Francais du Petrole.
[25] G. Franz, F. Heinrich, H.J. Ratajczak, US Patent 367 362, 1983, to Chemische Werke Huels Aktiengesellschaft.
[26] B. Juguin, J. Miquel, European Patent 66485, 1982, and US Patent 4434315, 1984, to Institut Francais du Petrole.
[27] B. Juguin, G. Martino, FR Patent 2 657605, 1991, to Institut Francais du Petrole.
[28] J.W. Myers, D.J. Strope, US Patent 4436949, 1984, to Phillips Petroleum Co.
[29] T.R. Hughes, H.M. White, R.J. White, J. Catal. 13 (1969) 58.
[30] H. Miyata, J.B. Moffat, J. Catal. 62 (1980) 357.
[31] T. Okuhara, N. Mizuno, M. Misono, Adv. Catal. 41 (1996) 113.
[32] T. Okuhara, Chem. Rev. 102 (2002) 3641.
[33] T. Okuhara, T. Nishimura, H. Watanabe, M. Misono, J. Mol. Catal. 74 (1992) 247.
[34] A. Miyaji, T. Echizen, K. Nagata, Y. Yoshinaga, T. Okuhara, J. Mol. Catal. A 201 (2003) 145.
[35] A. Miyaji, R. Ohnishi, T. Okuhara, Appl. Catal. A 262 (2004) 143.
[36] T. Sugii, R. Ohnishi, J. Zhang, A. Miyaji, Y. Kamiya, T. Okuhara, Catal. Today 116 (2006) 179.
[37] S. Gao, J.B. Moffat, Catal. Lett. 42 (1996) 105.
[38] S. Gao, J.B. Moffat, Colloids Surf. A 105 (1995) 133.
[39] B.B. Bardin, R.J. Davis, Appl. Catal. A 200 (2000) 219.
[40] E.P.L. Hunter, S.G. Lias, J. Phys. Chem. Ref. Data 27 (1998) 413.
[41] V. Gutmann, Coordination Chemistry in Non-Aqueous Solutions, Springer-Verlag, Wien/New York, 1968, pp. 19, 22.
[42] T. Okuhara, T. Yamada, K. Seki, K. Johkan, T. Nakato, Microporous Mesoporous Mater. 21 (1998) 637.
[43] M. Yoshimune, Y. Yoshinaga, T. Okuhara, Microporous Mesoporous Mater. 51 (2002) 165.
[44] N. Katada, H. Igi, J.H. Kim, M. Niwa, J. Phys. Chem. B 101 (1997) 5969.